Int J Biometeorol (2010) 54:131–139
DOI 10.1007/s00484-009-0261-0

ORIGINAL PAPER

Modelling radiation fluxes in simple and complex environments: basics of the RayMan model

Andreas Matzarakis · Frank Rutz · Helmut Mayer

Received: 22 April 2008 / Revised: 23 July 2009 / Accepted: 10 August 2009 / Published online: 12 September 2009

Abstract Short- and long-wave radiation flux densities absorbed by people have a significant influence on their energy balance. The heat effect of the absorbed radiation flux densities is parameterised by the mean radiant temperature. This paper presents the physical basis of the RayMan model, which simulates the short- and long-wave radiation flux densities from the three-dimensional surroundings in simple and complex environments. RayMan has the character of a freely available radiation and human-bioclimate model. The aim of the RayMan model is to calculate radiation flux densities, sunshine duration, shadow spaces and thermo-physiologically relevant assessment indices using only a limited number of meteorological and other input data. A comparison between measured and simulated values for global radiation and mean radiant temperature shows that the simulated data closely resemble measured data.

Keywords RayMan model · Radiation flux densities · Mean radiant temperature · Human-biometeorological indices · Human thermal comfort

Introduction

There is a strong demand in the field of applied sciences such as architecture, agriculture, and medicine, etc., for climatological and biometeorological methods and means of calculation that are easily understandable. The radiation and human-bioclimate model RayMan (Matzarakis et al. 2007) meets this demand. Despite its simplicity, RayMan provides good simulation results for radiation flux densities and thermo-physiologically significant assessment indices. Use of RayMan-derived results in applied sciences has many advantages (Mayer 1993; VDI 1998; Thorsson et al. 2004; Johansson and Emmanuel 2006; Matzarakis et al. 2007).

The human energy balance can be applied to the evaluation of the impact of the thermal component of climate on humans. This method has been used in several studies (e.g. Jendritzky et al. 1990; Höppe 1993; VDI 1998; Mayer et al. 2008). Under clear sky conditions in summer, short-wave radiation flux densities exhibit the greatest variation amongst all meteorological parameters, particularly in urban areas. The human-biometeorological influence of short- and long-wave radiation flux densities can be transferred into a synthetic parameter, the mean radiant temperature T_{mrt} (Jendritzky et al. 1990; Höppe 1993; Mayer 1993; VDI 1998). T_{mrt} is defined as the uniform temperature of a hypothetical spherical surface surrounding a human (emissivity $\varepsilon=1$) that would result in the same net radiation energy exchange with the subject as the actual, complex radiative environment. The latter usually varies considerably under open space conditions.

Existing methods for the calculation of short- and long-wave radiation flux densities are applied mostly to the analysis of radiation conditions at horizontal surfaces. For human-biometeorological studies, the radiation environment of the human body has to be considered in a three-dimensional way. Several models and software packages designed to calculate radiation and thermal comfort conditions in several ways and with various input possibilities now exist (ENVI-met, Bruse and Fleer 1998; Radtherm, www.thermoanalytics.com; Townscope, Teller and Azar 2001). In addition, methods for the calculation of short-wave radiation flux densities also exist. These techniques apply both simple and complex

A. Matzarakis (✉) · F. Rutz · H. Mayer
Meteorological Institute, Albert-Ludwigs-University of Freiburg,
Werthmannstrasse 10,
79085 Freiburg, Germany
e-mail: andreas.matzarakis@meteo.uni-freiburg.de

models with different time resolutions on the basis of different existing calculation methods (Valko 1966; Brühl and Zdunkowski 1983; Jessel 1983; Olseth and Skartveit 1993; VDI 1994; Badescu 1997; Ceballos and de Moura 1997; Meek 1997; Gul et al. 1998; Mora-Lopez and Sidrach-de-Cardona 1998; Kemmoku et al. 1999; Marki and Antonic 1999; Roderick 1999; Santamouris et al. 1999; Craggs et al. 2000; Gueymard 2000). Models using sunshine duration for the calculation of short-wave radiation flux densities are used (Valko 1966; Gopinathan 1992; Revfeim 1997; Sen 1998) as well as simple parameterisations for turbidity (Kasten 1980; Power 2001). Methods for the calculation of long-wave radiation flux densities are also available (Czeplak and Kasten 1987; Salsibury and D'Aria 1992; Diak et al. 2000; Nunez et al. 2000; Prata 1996; Iziomon and Mayer 2001; Iziomon et al. 2003). For complex situations in urban settings, several models and analytic methods are documented in the literature (Kaempfert 1949, 1951; Terjung and Louie 1974; Mohsen 1979; Frank et al. 1981; Zdunkowski and Brühl 1983; Littlefair 2001; Kanda et al. 2005).

The main purpose of this paper is to present a method for the simulation of T_{mrt} for thermal human-biometeorological studies on different space and time scales by use of the RayMan model. Additionally, sunshine duration and shadow in simple and complex environments are included in the model. The model is compatible with Windows® and can analyse complex urban structures and other environments. The model requires only basic meteorological data (air temperature, air humidity and wind speed) for the simulation of radiation flux densities and common thermal indices for the thermal human-bioclimate. In this paper, a comparison between results from possibilities of model runs and measurements is discussed.

Scientific background and methods

Mean radiant temperature

Cause and effect relations between the atmospheric environment and human health or human comfort can be analysed by a human-biometeorological classification (Kerslake 1972; ISO 1983; Jendritzky et al. 1990; VDI 1998; Matzarakis et al. 2007). The thermal component of the climate is an important factor and can be described and quantified in a thermo-physiologically significant way by thermal indices.

In summer, the mean radiant temperature T_{mrt} is the most significant meteorological input parameter for the human energy balance because of its modification by clouds as well as topographical and urban morphologies (Winslow et al. 1936; Clark and Edholm 1985). Therefore, T_{mrt} has the strongest influence on thermo-physiological significant indices like physiologically equivalent temperature (PET) or standard effective temperature (SET*; Mayer 1993; Gagge et al. 1986; Höppe 1999) in many climate environments. Here, the modelling/calculation of T_{mrt} only is presented.

For long-term studies without direct measurement of radiation flux densities, T_{mrt} can be simulated using models. In the literature, methods to estimate radiation flux densities based on parameters including air temperature, air humidity, degree of cloud cover, atmospheric turbidity, time of day, and day of the year are recommended (Jendritzky et al. 1990; Matzarakis et al. 2007). However, both the albedo of the surrounding surfaces and their solid angle proportions must be specified in these models. Additionally, other factors such as the geometrical properties of buildings, vegetation, reflexion properties, etc., have to be taken into account. For the application of such models in simple situations, the following radiation flux densities are required:

- direct solar radiation,
- diffuse solar radiation,
- reflected short-wave radiation,
- atmospheric radiation (long-wave) from the open sky,
- long-wave radiation from solid surfaces (lower hemisphere and horizon limitation).

The following parameters describing the surroundings of the human body must be known:

- sky view factor—because of the limitation of the horizon and the influence of short- and long-wave radiation flux densities,
- view factor of the different solid surfaces—because of the modification of the reflected short-wave radiation,
- albedo of the different solid surfaces—because of the influence of the incoming short-wave radiation,
- emissivity of the different solid surfaces—because of the influence on the surface temperature.

To calculate T_{mrt}, the entire surroundings of the human body are divided into n isothermal surfaces with the temperatures T_i (i=1 to n) and emissivities ε_i, for which the solid angle portions ("angle factors") F_i are used as weighting factors. Long-wave radiation ($E_i=\varepsilon_i*\sigma*T_i^4$) and diffuse short-wave radiation, D_i, are emitted from each of the n surfaces of the surroundings (Fanger 1972; Jendritzky et al. 1990). This results in an approach for T_{mrt} (Fanger 1972; Jendritzky and Nübler 1981) as:

$$T_{mrt} = \left[\frac{1}{\sigma}\sum_{i=1}^{n}\left(E_i + a_k\frac{D_i}{\varepsilon_p}\right)F_i\right]^{0.25} \quad (1)$$

where σ is the Stefan-Boltzmann constant [$5.67*10^{-8}$ W/(m^2K^4)] and ε_p is the emission coefficient of the human body (standard value 0.97). D_i comprises the diffuse solar radiation and the diffusely reflected global radiation, whereas

a_k is the absorption coefficient of the irradiated body surface area of short-wave radiation (standard value 0.7).

T_{mrt} is incremented to T^*_{mrt}, if there is also direct solar radiation (Jendritzky et al. 1990):

$$T^*_{mrt} = \left[T_{mrt}{}^4 + \frac{f_p a_k I^*}{(\varepsilon_p \sigma)} \right]^{0.25} \quad (2)$$

In this case, I* is the radiation intensity of the sun on a surface perpendicular to the incident radiation direction. The surface projection factor $f_p = 0.308\cos(\gamma(0.998 - \gamma^2)/50000)$ for the sun elevation angle γ (in degrees) is a function of the incident radiation direction and the body posture (VDI 1998, 2001; Jendritzky et al. 1990). For applications in human-biometeorology, it is generally sufficient to determine f_p for a rotationally symmetrical person standing or walking (Jendritzky et al. 1990).

Estimation of radiation fluxes and T_{mrt} by the RayMan model

The RayMan model is Windows-based software with the code written in Delphi. The model offers several estimation and input possibilities (described above and in Matzarakis et al. 2007). Here, only the method of estimation of the radiation flux densities and T_{mrt} is described. The model divides the three-dimensional environment into an upper and a lower hemisphere. Usually, the lower hemisphere has a sky view factor f_{svf} that is covered by solid surfaces. So, for the lower hemisphere the adjustment of the solid properties is easier than for the upper hemisphere. For the lower hemisphere, the albedo and emissivity have to been known in order to simulate the short- and long-wave radiation flux densities from the lower hemisphere (reflected short- and long-wave emission from the ground, see Fig. 1). The parting plane between the two hemispheres is at 1.1 m a.g.l., which represents the weighting centre of the human body (Fanger 1972; Jendritzky et al. 1990).

The distribution of the solid and free sky elements and their amount in the upper hemisphere are required for the estimation of the radiation flux density of the upper hemisphere. These elements can be attributed to a pixel map, e.g. of a fish-eye photograph (Fig. 2) or a rendered image of a vector model. Each pixel, p_i, in Fig. 2 corresponds to an angle factor F_i located at the azimuth angle α_i and the zenith angle ζ_i. The angle factor is weighted by $F_i = 1/(\pi N^2/4)\sin(\zeta_i)/\zeta_i$, where ζ_i is determined via $\zeta_i = \left(\Delta x_i^2 + \Delta y_i^2\right)^{1/2}\pi/N$ by the pixel distance Δx_i and Δy_i of p_i from the centre of the $N \times N$ pixels sized image in the x and y direction, respectively. Pixels with $\zeta_i > \pi/2$ (i.e. below the horizon) are ignored. Summing up all F_i values results in the sky view factor f_{svf}. T_{mrt} is obtained via Eqs. 1 and 2 together with the short- and long-wave radiation flux densities.

Estimation of global radiation

The global radiation G_o for undisturbed conditions (free horizon and no clouds) can be estimated as follows (Jendritzky et al. 1990; VDI 1994, 1998):

$$G_0 = 0.84 \cdot I_0 \cdot \cos\zeta \cdot \exp\left(-0.027 \cdot \frac{\rho}{\rho_0} \cdot T_L / \cos\zeta\right) \quad (3)$$

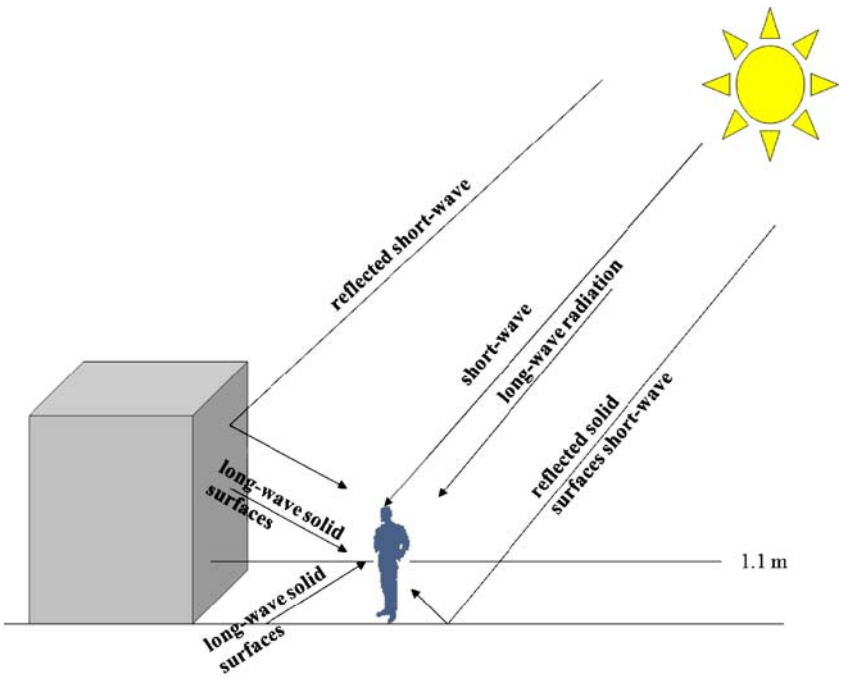

Fig. 1 Radiation flux densities important for the determination of the mean radiant temperature (T_{mrt})

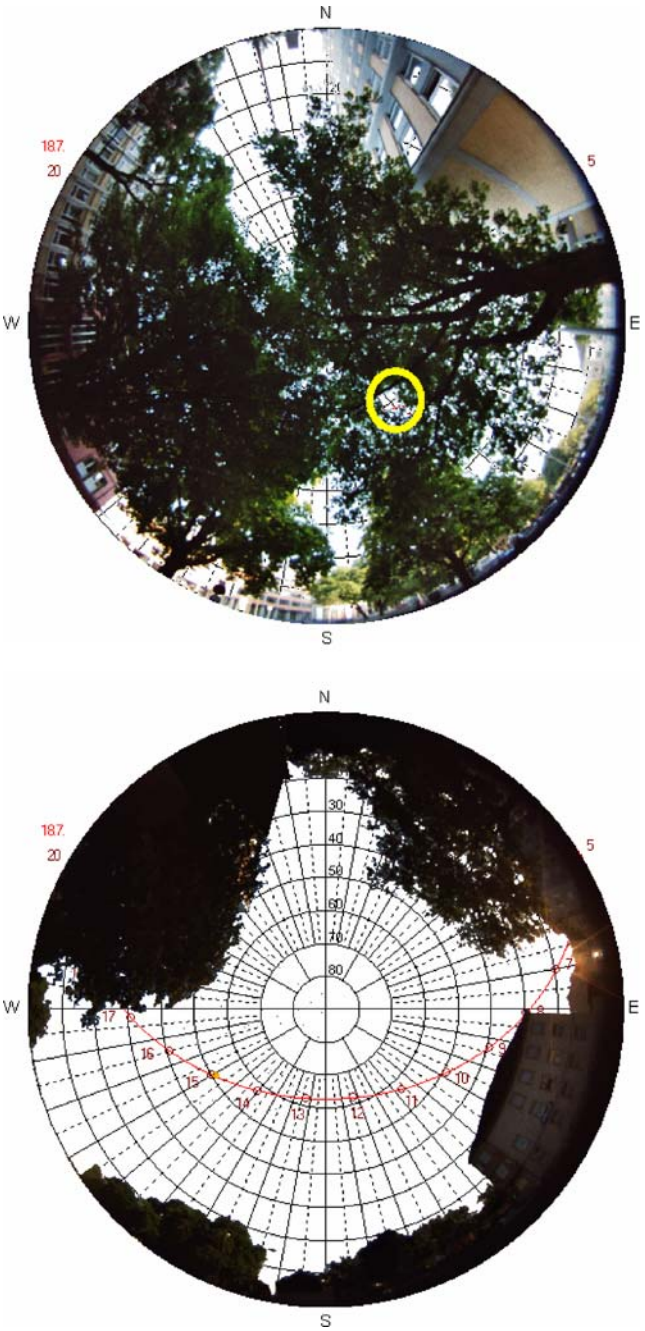

Fig. 2 Fish-eye photographs under the canopy of a group of trees (*upper*) and for a semi-open place (*lower*) in Freiburg. The *circle* in the upper image marks an opening in the tree crown

with the solar radiation flux density I_0 (W/m²), the zenith angle ζ (°) of the sun, the local atmospheric pressure p (hPa) relative to the normal pressure p_0=1,013 hPa at sea level, and the Linke turbidity factor T_L. However, for real-life applications this assumption is barely adequate. A better approach for G is the sum of the direct and the diffuse solar radiation, I and D, respectively, which both take horizon limitations and cloudiness into account.

For the direct radiation I on a horizontally oriented surface, the formulation is (Jendritzky et al. 1990):

$$I = I_0 \cdot \cos\zeta \cdot \exp\left(-T_L \cdot \delta_{r0} \cdot m_{r0} \cdot \frac{\rho}{\rho_0}\right) \cdot \left(1 - \frac{N}{8}\right) \quad (4)$$

if the sun is not masked by an obstacle. I_o is the irradiance of extraterrestrial solar radiation on the plane normal to the direction of incidence for the current solar distance (W/m^2). N denotes the degree of cloudiness in octas, δ_{op} the vertical optical thickness of the standard (Rayleigh) atmosphere, and m_{r0} the relative optical air mass, which considers the extended optical path through the atmosphere for zenith angles ζ>0 with respect to vertical incidence. Kasten and Young (1989) provided an equation for the relative optical air mass

$$m_{R0} = 1/\left(\sin\gamma + 0.50572 \cdot (\gamma + 6.07995°)^{-1.6364}\right) \quad (5)$$

with the solar altitude angle $\gamma = 90° - \zeta$. The optical thickness can be calculated (Kasten 1980) by

$$\delta_{R0} = 1/(0.9 m_{r0} + 9.4) \quad (6)$$

for zenith angles ζ<85° (i.e. γ>5°). For higher values of ζ (gazing incidence), an approximation according to Table 1 with linear interpolation for intermediate values satisfies. If the location of interest is in the shade, then I=0.

According to Valko (1966), the diffuse radiation can be composed linearly of the two extreme values for cloudless (N=0) and overcast (N=8) conditions:

$$D = D_0 \cdot \left(1 - \frac{N}{8}\right) + D_8 \cdot \frac{N}{8} \quad (7)$$

D_0, in turn, comprises an isotropic (D_{iso}) and an anisotropic (D_{aniso}) component, $D_0 = D_{iso} + D_{aniso}$. It holds that

$$D_{iso} = (G_0 - I(N=0)) \cdot (1 - \tau) \cdot f_{svf} \quad (8)$$

where $\tau = I(N=0)/(I_0 \cos\zeta)$ is the transmittance of the direct solar radiation represented by the exponential term in Eq. 4. f_{svf} allows for horizontal limitations due to the topo-

Table 1 Vertical optical thickness δ_{r0} for gazing incidence; intermediate values are interpolated linearly

γ	5°	4°	3°	2°	1°	0°
δ_{R0}	0.0548	0.0519	0.0491	0.0463	0.0435	0.0408

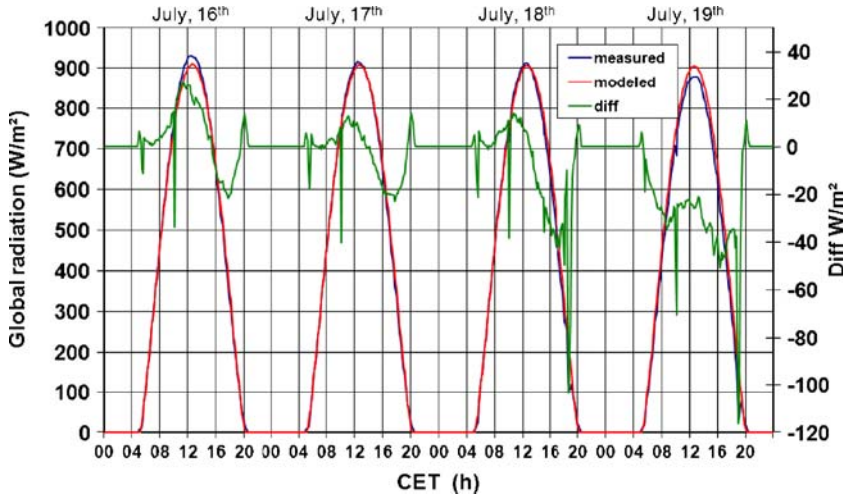

Fig. 3 Measured and simulated global radiation for 16–19 July 2006 in Freiburg, Germany

graphy, surrounding buildings, etc. Since the anisotropic radiation tends to concentrate in the vicinity of the sun, the calculation is discriminated depending on whether the sun is directly visible. Thus, no f_{svf} is taken into account in

$$D_{aniso} = (G_0 - I(N=0)) \cdot \tau \tag{9}$$

for the case where the sun is not hidden by the horizontal limitation, otherwise D_{aniso}=0. Finally, the (fully isotropic) overcast component is approximately

$$D_8 = G_0 \cdot (1 - 0.72) \cdot f_{svf} = 0.28\, G_0 \cdot f_{svf} \tag{10}$$

Estimation of atmospheric radiation

For the (long wave) atmospheric radiation, we used the Angstrom formula because it uses only general atmospheric parameters (air temperature and vapour pressure) and the mean cloud cover in octas without distinguishing between different cloud types and layers (Falkenberg and Bolz 1949; Monteith 1990; Oke 1987; VDI 1994):

$$A = \sigma \cdot T_a^4 \cdot \left(0.82 - 0.25 \cdot 10^{-0.0945 \cdot V_p}\right) \cdot \left(1 + 0.21 \cdot \left(\frac{N}{8}\right)^{2.5}\right) \tag{11}$$

Here, the air temperature T_{a} in K, the vapour pressure V_{p} in hPa and the degree of cloudiness N in octas are the required variables.

Estimation of the long-wave radiation flux density emitted by solid surfaces

Furthermore, the long-wave radiation E being emitted from solid surfaces can be expressed by

$$E = \varepsilon \cdot \sigma \cdot T_s^4 + (1 - \varepsilon) \cdot A \tag{12}$$

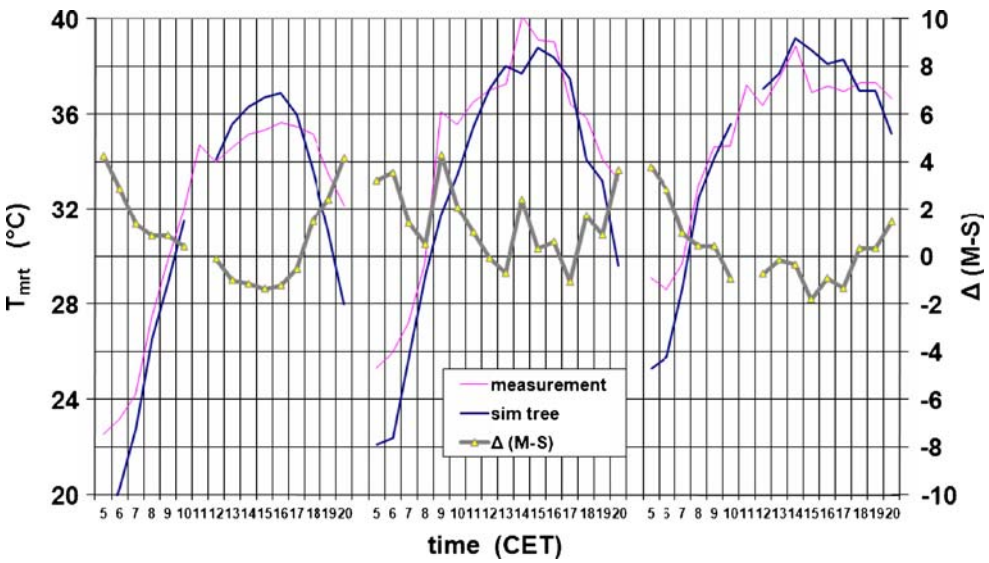

Fig. 4 Comparison between measured and simulated T_{mrt} for the period 17–19 July 2006 in Freiburg under the canopy of a group of trees [Δ (M−S) is difference between measurement and simulation]

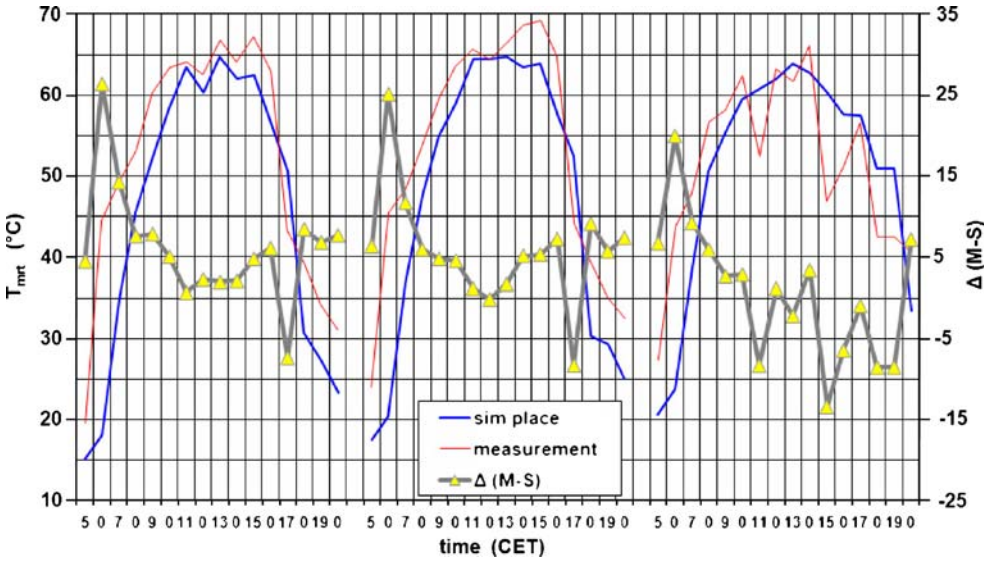

Fig. 5 Comparison between measured and simulated T_{mrt} for the period 17–19 July 2006 in Freiburg in a semi-open place [Δ (M−S) is difference between measurement and simulation]

The first part of the sum represents the thermal emission from a surface with temperature T_s (K). The second part is the non-absorbed (thus reflected) fraction of the incident long-wave radiation, which is dominated by the atmospheric radiation A in first approximation. The surface temperature can be initially estimated using air temperature and subsequently calculated (Oke 1987) via:

$$T_s = T_a + \frac{Q + B}{(6.2 + 4.26 \cdot v_{wind}) \cdot \left(1 + \frac{1}{B_O}\right)} \tag{13}$$

with the net all-wave radiation flux density Q, the soil flux B=−0.19 Q if Q>0 and −0.32 Q if Q<0, the wind velocity v_{wind} and the Bowen ratio B_o. Since $Q = a_k G + A - E$ incorporates E, both values E and T_s can be calculated iteratively with Eqs. 12 and 13. All energy flux densities are given in W m^{-2}.

Results

Validation of the model

RayMan has been tested in different environments, especially for studies with urban morphologies. It can be used for a range of purposes. In the following section, two tests of the RayMan model on different data sets are outlined.

The surroundings can be modelled basically in two ways: (1) by importing fish-eye photographs, and (2) by detailed description of obstacles such as buildings and trees by their geometrical properties (see Matzarakis et al. 2007). The vector model utilizes much more detailed information of the surroundings, which all has to be determined and declared.

In the following comparison, we used the fish-eye model since it is much easier to insert despite being the more complex means of estimating T_{mrt}.

Comparison of global radiation

Figure 3 presents the measured and simulated global radiation for four days in July 2006 (16–19) in Freiburg. The measured data are taken from the urban meteorological station Freiburg (Matzarakis and Mayer 2008) located on the roof of a tall building at 52 m a.g.l. in the northern part of the city of Freiburg. The simulated values for global radiation shown in Fig. 3 fit the measured values very well. Usually, the differences between modelled and measured global radiation range from −20 to +20 W/m^2 during sunshine hours and can be explained as an effect of turbidity. Thus, for the estimation of T_{mrt}, it is important to know the turbidity conditions. The differences increase

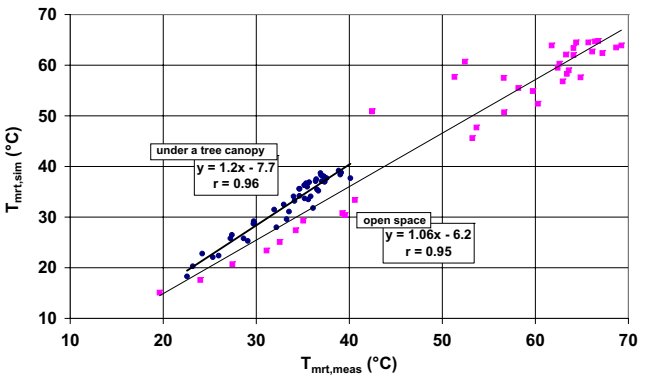

Fig. 6 Correlation between measured and simulated T_{mrt} values for the sites described in Fig. 4

to more than 20 W/m^2 (modelled) in the afternoon when clouds affect the measured global radiation. The one small negative peak in the morning hours (about 10:30 CET) is a result of the effect of the rope of the mast of the station.

Measured and modelled mean radiant temperature in urban areas

The accuracy of simulations of the mean radiant temperature T_{mrt} was tested over a period of 3 days in July 2006. The experimentally based determination of T_{mrt} used a combination of a pyranometer and a pyrgeometer according to Höppe (1993) and Matzarakis et al. (2007). Here, measured and simulated T_{mrt} are compared in two different environments. The fish-eye photos of the two points are shown in Fig. 2. The first point is under the canopy of a group of trees. Direct solar radiation, which can affect T_{mrt}, passes the tree canopy only between 11.00 and 12.00 CET (marked by the circle in Fig. 2). The second point is about 30 m away from the first point and is a semi-open location surrounded by buildings and trees. This measurement location is not affected by any obstacles between 8.00 and 17.00 CET. Thus, the comparison is better for time periods with direct solar radiation. When the sun is very close to the edges of obstacles (buildings), small error or variations by the fish-eye pictures and exact time influence the results exorbitantly. This leads to a pronounced scattering of data points at the times mentioned. Figure 4 shows the daily courses of the measured and simulated T_{mrt} under the tree canopy; both patterns are similar. The mean difference between measured and simulated T_{mrt} is less than 2°C. For the semi-open location (Fig. 5), the mean T_{mrt} difference shows a similar behaviour, with lower differences during times of high sun angle (between 10.00 and 15.00 CET from −6.4 to 6.1) with the highest measured value of 69.2°C. The highest differences occur at low sun angles in the morning and afternoon (−8.3 to 7.9°C). In general, the coefficient of determination, r, between measured and simulated T_{mrt} (Fig. 6) for the semi-open place is 0.95 [root mean square error (RMSE)=3.7 K] and for under the tree r is 0.96 (RMSE=0.7 K).

Discussion and conclusion

Comparison of T_{mrt} between measurements carried out at two locations in Freiburg (under trees and in semi-open space) shows that the differences under the tree canopy are low on average (less than 2°C). Only at low sun angles are the differences a little higher, particularly in the afternoon. This indicates that reflected radiation from vertical surfaces is not considered by the use of fish-eye photos. These effects become even more evident in the semi-open location, where differences during high sun angles are lower than in the late morning hours, during which the differences are higher (measured values are higher). This is because of the effect of the buildings and trees in the northern part of the space, which reflect radiation components. The additional reflection of these buildings (based on fish-eye photos) cannot be considered in the RayMan model, but these effects can be considered by the importance of their geometrical properties. On the one hand, short-wave radiation flux densities in complex environments are highly influenced by the reflection of obstacles. These effects can be seen in the morning hours and sometimes during midday in the semi-open space. Thorsson et al. (2007) found similar effects in their comparison. On the other hand, the simulated data for global radiation and also for the T_{mrt} closely resemble the measured data (for both simple and complex environments with regards to global radiation properties).

Based on the comparison results it can be concluded that the RayMan model (based on fish-eye photos and geometrical properties of the surroundings) is a suitable tool for the simulation of radiation flux densities and T_{mrt}, which are required for thermal comfort studies and related studies. Another advantage of the model is the short running time in comparison with other models. Note also that, in semi-open locations, the differences between measured and simulated T_{mrt} are lower if the surroundings are based on truly geometrical properties.

The development of the RayMan model is not yet complete. It is planned to continue the development of RayMan, especially with regard to the import of computer-aided design (CAD) files and digital atlas data, which will allow a more straightforward calculation of the geometrical properties of urban structures and obstacles.

In general, there is a strong demand for human-biometeorological and urban climate models, not only in this research area itself, but also from urban planners and architects. The end users of the model obviously prefer easily understandable models that require only limited input data. RayMan is available for general use under (http://www.urbanclimate.net/rayman) and has an easy user-friendly interface.

Acknowledgements Thanks a million to RayMan users for their suggestions and validations. Both represent the basis for further development of the model.

References

Badescu V (1997) Verification of some very simple clear and cloudy sky model to evaluate global solar irradiance. Sol Energy 61:251–264

Brühl Ch, Zdunkowski W (1983) An approximate calculation method for parallel and diffuse solar irradiances on inclined surfaces in the presence of obstructing mountain or buildings. Arch Meteorol Geophys Bioclimatol B 32:111–129

Bruse M, Fleer H (1998) Simulating surface-plant-air interactions inside urban environments with a three dimensional numerical model. Environ Model Softw 13:373–384

Ceballos JC, Moura GB de A (1997) Solar irradiation assessment using meteosat 4-Vis imagery. Solar Energy 60:209–219

Clark RP, Edholm OG (1985) Man and his thermal environment. Arnold, London

Craggs C, Conway EM, Pearsall NM (2000) Statistical investigation of the optimal averaging time for solar irradiance on horizontal and vertical surfaces in the UK. Sol Energy 68:79–187

Czeplak G, Kasten F (1987) Parametrisierung der atmosphärischen Wärmestrahlung bei bewölktem Himmel. Meteorol Rdsch 40: 184–187

Diak GR, Bland WL, Mecikalski JR, Anderson MC (2000) Satellite-based estimates of longwave radiation for agricultural applications. Agric For Meteorol 103:349–355

Falkenberg G, Bolz HM (1949) Neue Bestimmung der Konstanten der Angströmschen Strahlungsformel. Z Meteorol 3:97

Fanger PO (1972) Thermal comfort. McGraw-Hill, New York

Frank SF, Gerding RB, O'Rourke PA, Terhung WH (1981) An urban radiation obstruction model. Bound-Lay Meteorol 20:259–264

Gagge AP, Fobelets AP, Berglund LG (1986) A standard predictiveindex of human response to the thermal environment. ASHRAETrans 92:709–731

Gopinathan KK (1992) Estimation of hourly global radiation and diffuse solar radiation from hourly sunshine duration. Sol Energy 48:3–5

Gueymard C (2000) Prediction and performance assessment of mean hourly global radiation. Sol Energy 68:285–303

Gul MS, Muneer T, Kambezidis HD (1998) Models for obtaining solar radiation from other meteorological data. Sol Energy 64: 99–108

Höppe P (1993) Heat balance modelling. Experientia 49:741–746

Höppe P (1999) The physiological equivalent temperature—a universal index for the biometeorological assessment of the thermal environment. Int J Biometeorol 43:71–75

ISO (1983) ISO 7730: Moderate thermal environments—Determination of the PMV and PPD indices and specification of the conditions of thermal comfort. International Organization for Standardization, Geneva

Iziomon MG, Mayer H (2001) Performance of solar radiation models—a case study. Agric For Meteorol 110:1–11

Iziomon MG, Mayer H, Matzarakis A (2003) Downward atmospheric longwave irradiance under clear and cloudy skies: Measurement and parameterization. J Atmos Sol-Terr Phys 65:1107–1116

Jendritzky G, Nübler W (1981) A model analysing the urban thermal environment in physiologically significant terms. Arch Meteorol Geophys Bioclimatol B 29:313–326

Jendritzky G, Menz H, Schirmer H, Schmidt-Kessen W (1990) Methodik zur raumbezogenen Bewertung der thermischen Komponente im Bioklima des Menschen (Fortgeschriebenes Klima-Michel-Modell). Beitr Akad Raumforsch Landesplan, No. 114

Jessel W (1983) Die diffuse Himmelstrahlung. Eine vergleichende Darstellung der Bestrahlungsstärke bezogen auf eine kugelförmige und eine ebene horizontale Empfangsfläche. Arch Meteorol Geophys Bioclimatol B 32:23–52

Johansson E, Emmanuel R (2006) The influence of urban design on outdoor thermal comfort in the hot, humid city of Colombo, Sri Lanka. Int J Biometeorol 51:119–133

Kaempfert W (1949) Zur Frage der Besonnung enger Strassen. Meteorol Rdsch 2:222–227

Kaempfert W (1951) Ein Phasendiagramm der Besonnung. Meteorol Rdsch 4:141–144

Kanda M, Kawai T, Nagakawa K (2005) A simple theoretical radiation scheme for regular building arrays. Bound-Lay Meteorol 114: 71–90

Kasten F (1980) A simple parametrization of the pyrheliometric formula for determining the Linke turbidity factor. Meteorol Rdsch 33:124–127

Kasten F, Young AT (1989) Revised optical air mass tables and approximation formula. Appl Optics 28:4735–4738

Kemmoku Y, Orita S, Nakagawa S, Sakakibara T (1999) Daily insolation forecasting using a multi-stage neural network. Sol Energy 66:193–199

Kerslake D McK (1972) The stress of hot environments. Cambridge University Press, Cambridge

Littlefair P (2001) Daylight, sunlight and solar gain in the urban environment. Sol Energy 70:177–185

Marki A, Antonic O (1999) Annual models of monthly mean hourly direct, diffuse, and global radiation at ground. Meteorol Z NF 8:91–95

Matzarakis A, Mayer H (2008) Importance of urban meteorological stations—the example of Freiburg, Germany. In: Mayer H (ed) Celebrating the 50Years of the Meteorological Institute, Albert-Ludwigs-University ofFreiburg, Germany. Ber Meteorol Inst Univ Freiburg Nr. 17, pp 101–110

Matzarakis A, Rutz F, Mayer H (2007) Modelling radiation fluxes in simple and complex environments—application of the RayMan model. Int J Biometeorol 51:323–334

Mayer H (1993) Urban bioclimatology. Experientia 49:957–963

Mayer H, Holst J, Dostal P, Imbery F, Schindler D (2008) Human thermal comfort in summer within an urban street canyon in Central Europe. Meteorol Z 17:241–250

Meek DW (1997) Estimation of maximum possible daily global radiation. Agric For Meteorol 87:223–241

Mohsen MA (1979) Solar radiation and courtyard house forms—I. A mathematical model. Build Environ 14:89–106

Mora-Lopez LL, Sidrach-de-Cardona M (1998) Multicaptive arma models to generate hourly series of global irradiation. Sol Energy 63:283–291

Monteith JL, Unsworth M (1990) Principles of environmental physics, 2nd edn. Elsevier, Oxford

Nunez M, Eliasson I, Lindgren J (2000) Spatial variation of incoming longwave radiation in Göteborg, Sweden. Theor Appl Climatol 67:181–192

Oke TR (1987) Boundary layer climates. Methuen, London

Olseth JA, Skartveit A (1993) Characteristics of hourly global irradiance modelled from cloud data. Sol Energy 51:197–204

Power H (2001) Estimating atmospheric turbidity from climate data. Atmos Environ 35:125–134

Prata AJ (1996) A new long-wave formula for estimating downward clear-sky radiation at the surface. Q J R Meteorol Soc 122:1127–1151

Revfeim KJA (1997) On the relationship between radiation and mean daily sunshine. Agric For Meteorol 86:183–191

Roderick ML (1999) Estimating the diffuse component from daily and monthly measurements of global radiation. Agric For Meteorol 95:169–185

Salsibury JW, D'Aria DM (1992) Emissivity of terrestrial material in the 8–14 μm atmospheric window. Remote Sens Environ 42:83–106

Santamouris M, Mihalakakou G, Psiloglou B, Eftaxias G, Asimakopoulos DN (1999) Modeling the global irradiation on the earth´s surface using atmospheric deterministic and intelligent data-driven techniques. J Climate 12:3105–3116

Sen Z (1998) Fuzzy algorithm for estimation of solar radiation from sunshine duration. Sol Energy 63:39–49

Teller J, Azar S (2001) Townscope II—a computer system to support solar access decision-making. Sol Energy 70:187–200

Terjung WH, Louie S (1974) A climatic model of urban energy budgets. Geogr Anal 6:341–367

Thorsson S, Lindqvist M, Lindqvist S (2004) Thermal bioclimatic conditions and patterns of behaviour in an urban park in Göteborg, Sweden. Int J Biometeorol 48:149–156

Thorsson S, Lindberg F, Eliasson I, Holmer B (2007) Different methods for estimating the mean radiant temperature in an outdoor urban setting. Int J Climatol 27:1983–1993

Valko P (1966) Die Himmelsstrahlung in ihrer Beziehung zu verschiedenen Parametern. Arch Meteorol Geophys Bioclimatol B14:337–359

VDI (1994) VDI 3789, Part 2: Environmental meteorology. Interactions between atmosphere and surfaces; calculation of the short- and long wave radiation. Beuth, Berlin

VDI (1998) VDI 3787, Part I: Environmental Meteorology, Methods for the human biometeorological evaluation of climate and air quality for the urban and regional planning at regional level. Part I: Climate. Beuth, Berlin

VDI (2001) VDI 3789, Part 3: Environmental Meteorology, interactions between atmosphere and surfaces; calculation of spectral irradiances in the solar wavelength range. Beuth, Berlin

Winslow CEA, Herrington LP, Gagge AP (1936) A new method of particional calorimetry. Am J Physiol 116:641–655

Zdunkowski W, Brühl Ch (1983) A fast approximate method for the calculation of the infrared radiation balance within city street cavities. Arch Meteorol Geophys Bioclimatol B 33:237–241